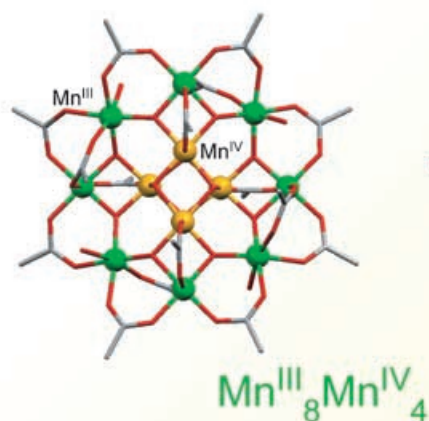
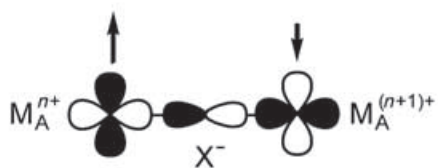


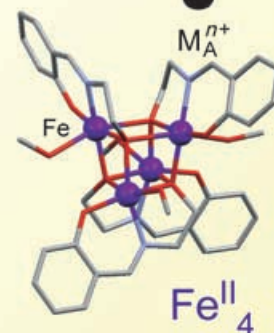
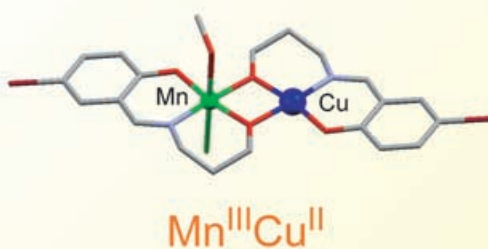
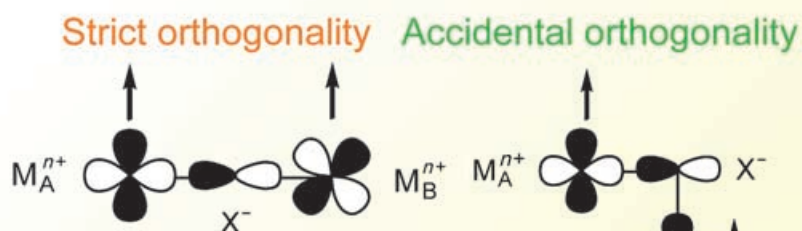
High-Spin Molecules with Magnetic Anisotropy toward Single-Molecule Magnets

High-Spin Molecules

Antiferromagnetic interaction

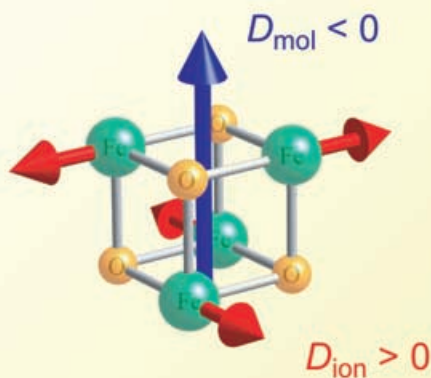


Ferromagnetic interaction

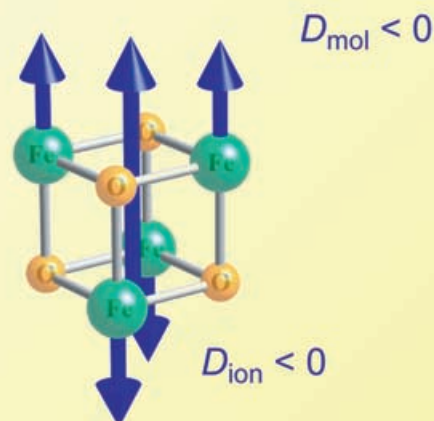


Molecules with Negative D Values

Orthogonal hard-axis alignment



Collinear easy-axis alignment



High-Spin Molecules with Magnetic Anisotropy toward Single-Molecule Magnets

Hiroki Oshio*^[a] and Motohiro Nakano^[b]

Abstract: High-spin molecules with easy-axis magnetic anisotropy show slow magnetic relaxation of spin-flipping along the axis of magnetic anisotropy and are called single-molecule magnets (SMMs). SMMs behave as molecular-size permanent magnets at low temperature and magnetic relaxation occurs by quantum tunneling processes; such molecules are promising candidates for use in quantum devices. We first discuss intramolecular ferromagnetic interactions for preparing high-spin molecules. Second, we determine the magnetic anisotropy for single metal ions with d^n configurations and discuss how molecular anisotropy arises from single-ion anisotropy of the assembled component metal ions.

Keywords: heterometallic complexes • high-spin molecules • magnetic properties • single-molecule studies

Introduction

Paramagnetic metal complexes have been thoroughly investigated with respect to their catalytic, biochemical, and physical properties, and a number of recent studies involve high-spin molecules with easy-axis-type magnetic anisotropy. These high-spin molecules have an energy barrier preventing easy reversal of the magnetic moment. They show slow magnetic relaxation with respect to spin flipping along the magnetic anisotropy axis, and at very low temperatures the

spin cannot thermally flip, but flips by means of quantum processes. Thus, the high-spin molecules behave as if they are molecular-size permanent magnets. Molecules that have this superparamagnetic behavior are called single-molecule magnets (SMMs).^[1] Since the discovery of the first SMM, a manganese-oxo cluster $[Mn_{12}]$,^[2] several types of SMMs have been reported,^[3] and recently larger size SMMs have been prepared with hope that novel physical properties might appear on the border between mesoscopic and bulk systems.^[4] Studies involving quantum tunneling of the magnetization^[5] and quantum phase interference^[6] have been conducted with the hope of using SMMs in quantum devices in the future.^[7] SMMs are required to possess a high-spin ground state and magnetic anisotropy to trap molecular magnetization. First, we discuss strategies for preparing high-spin molecules with intramolecular ferromagnetic interactions. Second, we will review magnetic anisotropy of single metal ions with d^n configurations and discuss how molecular magnetic anisotropy arises due to the arrangements of the constituent anisotropic metal ions. Molecular magnetic anisotropy, which mainly comes from single-ion anisotropy, should be easy-axis rather than easy-plane type in SMMs. A simple ligand field approach gives some insights into single-ion magnetic anisotropy.^[8]

Discussion

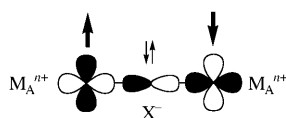
High-spin molecule with ferromagnetic interactions: For cluster molecules to be classified as SMMs, they must have a large uniaxial easy-axis type of magnetic anisotropy and a large ground-state spin multiplicity. Different strategies need to be used in order to prepare high-spin molecules composed of hetero- and homometal complexes. In heterometal systems, antiferromagnetic interactions lead to a ferromagnetic high-spin ground state, and this strategy has been used often to prepare SMMs. In homometal systems ferromagnetic interactions tend to have a higher spin ground state, although spin-frustrated, spin-canted, and mixed-valent homometal systems have lower spins. Ferromagnetic

[a] Prof. H. Oshio
Graduate School of Pure and Applied Sciences
Department of Chemistry, University of Tsukuba
Tennodai 1-1-1, Tsukuba 305-8571 (Japan)
Fax: (+81)298-53-4238
E-mail: oshio@chem.tsukuba.ac.jp

[b] Dr. M. Nakano
Department of Applied Chemistry
Graduate School of Engineering, Osaka University, 2-1
Yamadaoka, Suita, Osaka 565-0871 (Japan)

spin systems must be designed with special care, or the molecules have low-spin ground states.

Paramagnetic metal ions in a molecule are subject to magnetic interactions through superexchange and/or spin polarization mechanisms, among which the superexchange mechanism is predominant in metal complexes bridged by single anions. Superexchange interactions are mediated by charge-transfer (CT) interactions between metal ions and bridging ligands. Isotropic superexchange interaction is expressed by the spin Hamiltonian, $H = -2\sum J_{ij}S_iS_j$, in which J is the exchange coupling constant and a positive J value means the occurrence of ferromagnetic interactions. The superexchange mechanism, proposed by Anderson, Goodenough, and Kanamori,^[9] can be used to predict the sign of the J values. When two homometal ions are bridged by an anion with a bridging angle of 180°, for example, strong antiferromagnetic interactions ($J < 0$) occur through ligand-to-metal (LM) CT interactions and a low-spin ground state is stabilized (Scheme 1). For example, if metal ion on the left in the

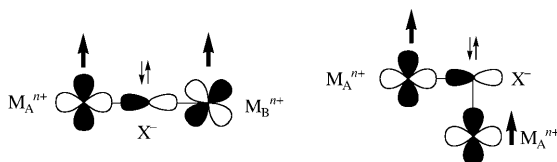


Scheme 1.

dinuclear system shown in Scheme 1 has an “up” spin, the LMCT interaction transfers a “down”-spin electron from the central anion to this metal ion, leaving an “up” spin on the anion. The remaining “up” spin on the anion stabilizes the “down” spin on the right-hand metal ion, and this situation leads to the occurrence of the antiferromagnetic interaction. There are a few exceptions of this rule for complexes in which metal ions have spins on degenerate orbitals. For linearly oxo-bridged V^{III} dimers ferromagnetic interactions are observed, which have been explained by a kinetic exchange mechanism.^[10]

Magnetic interactions between bridged metal ions are typically antiferromagnetic. There are, however, two ways that ferromagnetic interactions for hetero- and homometal systems can occur (Scheme 2).

- 1) A combination of heterometal ions, each with orthogonal magnetic orbitals, leads to the ferromagnetic interaction.



Strict orthogonality

Accidental orthogonality

Scheme 2.

tions. A strong ferromagnetic interaction was reported for a [Cu–V=O] complex (Figure 1, top), in which strict orthogonality of the metal ions (dσ and dπ spins for Cu and V=O ions, respectively) is responsible for the occurrence of the ferromagnetic interaction.^[11]

- 2) When homometal ions are linked without magnetic orbital overlaps, a high-spin ground state occurs. Metal ions bridged with a bond angle of 90° have ferromagnetic interactions, and a high-spin ground state is observed.

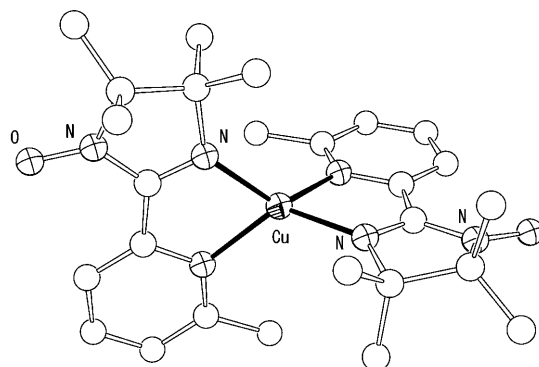
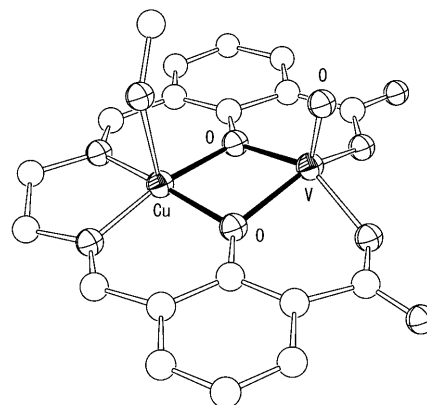


Figure 1. ORTEP drawings of dinuclear Cu^{II}–V=O (top)^[10a] and bis-iminonitroxyl Cu^I (bottom)^[11] complexes showing ferromagnetic interactions.

A relatively strong ferromagnetic interaction was observed between two iminonitroxyl radicals orthogonally linked by a copper(I) ion (Figure 1, bottom), which favors a tetrahedral coordination geometry and causes an orthogonal arrangement (dihedral angle of 90°) of magnetic orbitals on the coordinated bidentate ligand.^[12] Phenoxo and alkoxo groups sometime bridge metal ions without magnetic orbital overlaps (bridging bond angle close to 90°), leading to ferromagnetic interactions.^[13] It should be noted that CT interactions play very important roles in the propagation of magnetic interactions, and weak magnetic interactions due to magnetic dipolar interactions are operative without the CT interaction.

Magnetic anisotropy: Molecules with easy-axis-type zero-field splitting ($D_{\text{mol}} < 0$) have a double minimum potential

with an energy barrier profile of $D_{\text{mol}}S_z^2$ at the inversion of the magnetic moment from $S_z = +S$ to $-S$. These high-spin molecules show slow magnetic relaxation of the spin flipping at very low temperature. The spin Hamiltonian is defined in Equation (1) in which the first term represents the Zeeman energy, and the second and third terms are contributions from the magnetic anisotropies of uniaxial (D_{mol}) and rhombic (E_{mol}) zero-field splittings, respectively.

$$\hat{H} = -g\mu_B H \hat{S} + D_{\text{mol}}[\hat{S}_z^2 - S(S+1)/3] + E_{\text{mol}}(\hat{S}_x^2 - \hat{S}_y^2) \quad (1)$$

Magnetic anisotropy of paramagnetic molecules occurs due to several factors including single-ion anisotropy of the constituent metal ions, anisotropic exchange interactions between these ions, and magnetic dipolar interactions. Among them, single-ion anisotropy often dominates molecular anisotropy. Chemists are mostly interested in how molecular anisotropy arises from single-ion anisotropy through molecular architecture. Before proceeding to the construction of molecular anisotropy, magnetic anisotropy for a single ion is reviewed within conventional ligand-field theory.

Magnetic anisotropy for a single metal ion: The sign of single-ion D values depends upon the electron configuration and ligand-field environment of the metal ion. The electronic ground state of a transition metal ion is usually represented with a term symbol, which transforms as an irreducible representation of the point group reflecting the molecular symmetry. Table 1 summarizes the ground states of high-

Table 1. Electronic ground states of transition metal ions under O_h and D_{4h} environments.^[a]

	d ¹	d ²	d ³	d ⁴	d ⁵	d ⁶	d ⁷	d ⁸	d ⁹
elongated D_{4h}	² E _g	³ A _{2g} (+)	⁴ B _{1g} (+)	⁵ B _{1g} (−)	⁶ A _{1g} (+)	⁵ E _g	⁴ A _{2g} (+)	³ B _{1g} (+)	² B _{1g}
octahedral O_h	² T _{2g}	³ T _{1g}	⁴ A _{2g}	⁵ E _g	⁶ A _{1g}	⁵ T _{2g}	⁴ T _{1g}	³ A _{2g}	² E _g
compressed D_{4h}	² B _{2g}	³ E _g	⁴ B _{1g} (−)	⁵ A _{1g} (+)	⁶ A _{1g} (−)	⁵ B _{2g} (+)	⁴ E _g	³ B _{1g} (−)	² A _{1g}

[a] Metal ions with d⁴–d⁷ configurations are in the high-spin states. (+) and (−) signs denote ions possessing positive and negative D values, respectively, if the ground state is not a Kramers doublet and the orbital degeneracy is fully quenched.

spin dⁿ metal ions under O_h and D_{4h} symmetry. The ^{2S+1}T and ^{2S+1}E electronic ground terms under O_h symmetry are often unstable towards distortion of the coordination sphere which breaks the symmetry (Jahn–Teller effect).

When the orbital degeneracy is completely lifted in the electronic ground state under a low-symmetry ligand field, the Abragam–Pryce's derivation of the spin Hamiltonian can be used to define the zero-field splittings as the quadratic forms of the spin operators including uniaxial D and rhombic E terms [Eqs. (2) and (3)],^[14] in which λ and $A_{\alpha\beta}$ are the spin-orbit coupling constant and the mixing tensor of the ground and excited states.

$$D = \lambda^2(A_{xx} + A_{yy} - 2A_{zz})/2 \quad (2a)$$

$$E = \lambda^2(A_{xx} - A_{yy})/2 \quad (2b)$$

$$A_{\alpha\beta} = \sum_{n \neq 0} \frac{\langle \varphi_0 | \hat{L}_\alpha | \varphi_n \rangle \langle \varphi_n | \hat{L}_\beta | \varphi_0 \rangle}{E_n - E_0} \quad (3)$$

The sign of the D value depends upon the relative amplitude of $A_{\alpha\beta}$. These anisotropy terms originate from spin-orbit coupling $\lambda \mathbf{L} \cdot \mathbf{S}$, which mixes higher energy multiplets into the ground state by means of second-order perturbations, and they dominate low-temperature magnetism of transition metal complexes that are either easy-axis type with negative D or easy-plane type with positive D . On the other hand, because the zero-field splittings in degenerate ground states are more complicated and cannot be expressed in terms of simple D and E parameterization, the magnetic anisotropies of those ions are not identified by the sign of the D parameters. Instead, the easy-axis or easy-plane anisotropies are found in the difference between longitudinal and transverse Zeeman effects if the lowest sub-levels are not extremely diamagnetic. For example, the E_g states under D_{4h} symmetry in Table 1 (compressed d², elongated d⁶, and compressed d⁷) are all easy-axis type with a large parallel component of the g tensor. Of course, most doubly degenerate ground states in metal complex molecules split to give a nondegenerate ground state with lower symmetry perturbations, and, therefore, the anisotropies can be described in terms of the parameters D and E .

The energy level diagrams for d¹–d⁹ electron configurations under low-symmetry ligand field were calculated by using the angular overlap model (AOM).^[15] The full Hamiltonian can be expressed as the sum of ligand field (H_{LF}), spin-orbit coupling (H_{LS}), electron repulsion (H_{ee}) and Zeeman (H_{Z}) terms as given in Equations (4)–(7),^[16] in which N_L , e_σ or $\pi(i)$, Ω_i , F_{e_σ} or t_{2g} , k , g_e , and ζ represent the coordination number, the AOM parameters and Eulerian angle of i -th ligand atom, the overlap factor between metal d and ligand orbitals, the Stevens' orbital reduction factor, the Landé g factor for a free electron, and the spin-orbit coupling constant, respectively.

$$\hat{H} = \hat{H}_{\text{LF}} + \hat{H}_{\text{LS}} + \hat{H}_{\text{ee}} + \hat{H}_{\text{Z}} \quad (4)$$

$$\begin{aligned} \hat{H}_{\text{LF}} = & \sum_{i=1}^{N_L} [e_\sigma(i) \sum_{e_g} \sum_{e'_g} |e_g\rangle F_{e_g}(\Omega_i) F_{e'_g}(\Omega_i) \langle e'_g| + \\ & e_\pi^\parallel(i) \sum_{t_{2g}} \sum_{t'_{2g}} |t_{2g}\rangle F_{t_{2g}}^\parallel(\Omega_i) F_{t'_{2g}}^\parallel(\Omega_i) \langle t'_{2g}| + \\ & e_\pi^\perp(i) \sum_{t_{2g}} \sum_{t'_{2g}} |t_{2g}\rangle F_{t_{2g}}^\perp(\Omega_i) F_{t'_{2g}}^\perp(\Omega_i) \langle t'_{2g}|] \end{aligned} \quad (5)$$

$$\hat{H}_{\text{LS}} = k \sum_i \zeta \cdot \hat{l}_i \cdot \hat{s}_i \quad (6)$$

$$\hat{H}_{ee} = \frac{1}{4\pi\epsilon_0} \sum_{i>j} \frac{e^2}{|r_i - r_j|} \quad (7)$$

$$\hat{H}_z = -\mu_B(k\hat{L} + g_e\hat{S}) \cdot H$$

The values of the ligand-field strengths and other model parameters used in the AOM calculations, which were chosen from physically reasonable range referring to the references,^[15] are summarized in the caption for Figure 2. The

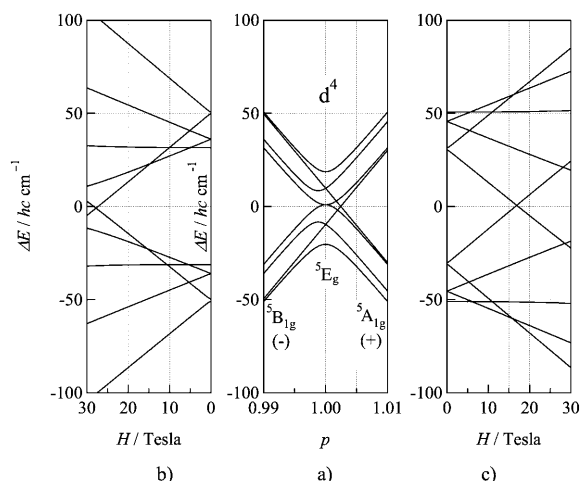


Figure 2. a) Energy splitting diagram calculated for a six-coordinate 3d⁴ system with ML₆ conformation. The scaling factor *p* changes the axial ligand-field strengths of *e_π* and *e_σ*. *O_h* symmetry has a *p* parameter of 1.0, while compressed and elongated forms have *p* > 1 and *p* < 1, respectively. Ligand-field strengths: *e_σ* = 4000 cm⁻¹ and *e_π* = 1200 cm⁻¹; Racah parameters: *B*/*h*c = 600.0 cm⁻¹ and *C*/*B* = 4.3; Spin-orbit coupling constant: *ζ*/*h*c = 400.0 cm⁻¹; Stevens' orbital reduction factor: *k* = 0.7.^[15] (+) and (-) signs represent positive and negative *D* values, respectively. Zeeman splitting schemes by the applied magnetic field parallel to the apical axis at b) *p* = 0.99 (elongated form) and c) *p* = 1.01 (compressed form).

σ and *π* characters of the ligand atoms are measured by *e_σ* and *e_π* parameters. The symmetry lowering of the *O_h* ligand field is expressed by introducing a scaling factor *p*, which modulates both *e_σ* and *e_π* of the axial ligands, keeping the equatorial ligand field unchanged. Deviation of *p* from unity corresponds to either compressed (*p* > 1) or elongated (*p* < 1) octahedral coordination. The results for ground multiplet splittings for each state under *D_{4h}* symmetry (ML₆) are shown in Figures 2–4.

First, we discuss Mn^{III} (3d⁴) ions, which have been used often to prepare SMMs. The calculated energy splitting scheme for the 3d⁴ system is

shown in Figure 2a. A Mn^{III} ion with *O_h* symmetry has a ⁵E_g ground state, which splits to provide ⁵B_{1g} and ⁵A_{1g} ground states under tetragonal elongation (*p* < 1) and compression (*p* > 1) of the coordination sphere, respectively (Jahn–Teller effect). The ⁵A_{1g} term has two quasi-twofold degenerate sublevels above the nondegenerate ground sublevel, which is well-described by positive *D*. The ⁵B_{1g} term has the inverted sublevel structure corresponding to negative *D* (Figure 2). This was proven by calculations with the magnetic field applied along the apical axis. The Zeeman effect for these ground multiplets clearly confirms the sign of uniaxial zero-field splitting parameter *D*. When the axial *π* and *σ* donations is weaker than equatorial ones (elongated form with *p* < 1), the ⁵B_{1g} term shows quasi-first-order Zeeman splitting into *M_s* = ±2, ±1, and 0 in order from the lowest energy (Figure 2b), suggesting negative *D* values (Figure 2b). When axial donation is stronger (*p* > 1), the ⁵A_{1g} state splits into five states, and the two sets of the higher energy states show Zeeman splitting by the magnetic field along the apical axis (Figure 2c). The lowest state was assigned to the *M_s* = 0 state, which corresponds to a positive value of *D* for the axially compressed Mn^{III} ion (Figure 2c).

Energy splitting diagrams of metal ions with high-spin d^{*n*} electron configurations are shown in Figures 3 and 4, and Table 1 lists the sign of *D* values for orbitally nondegenerate terms. Orbitally degenerate terms (Figure 3) have large splittings due to the first order perturbation of the spin-orbit coupling, while orbitally nondegenerate terms (Figure 4) such as ^{2S+1}A terms in the d³, d⁵, and d⁸ electron configurations have a small amount of splitting because of mixing with higher energy terms.

Degenerate orbital terms have more complicated zero-field splitting, which is very sensitive to ligand-field distortion. Energy splittings of a ⁵E_g term for a d⁶ electron configuration were calculated as a variable *p'* representing rhombic distortion from an axially elongated system, whereby the parameter *p* was fixed to 0.9. The results were shown in Figure 5, left. In this situation, the ligand-field strengths along three coordination axes (*x*, *y*, and *z*) have the ratio of

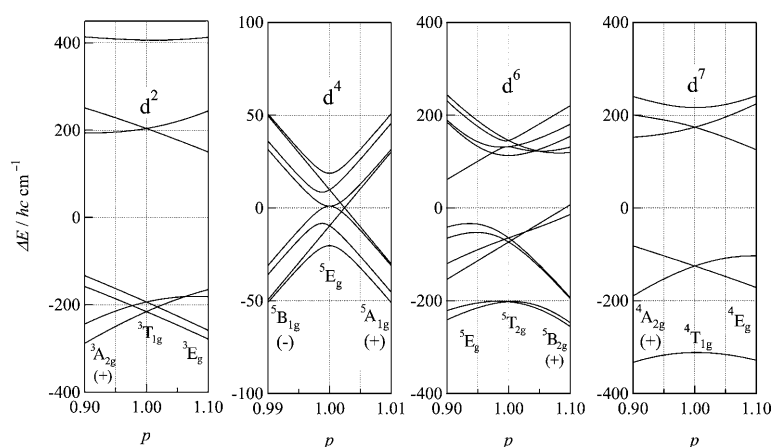


Figure 3. Energy splitting diagrams calculated for 3d², 3d⁴, 3d⁶, and 3d⁷ systems with ML₆ coordination. The parameters used in the calculations are summarized in Figure 2.

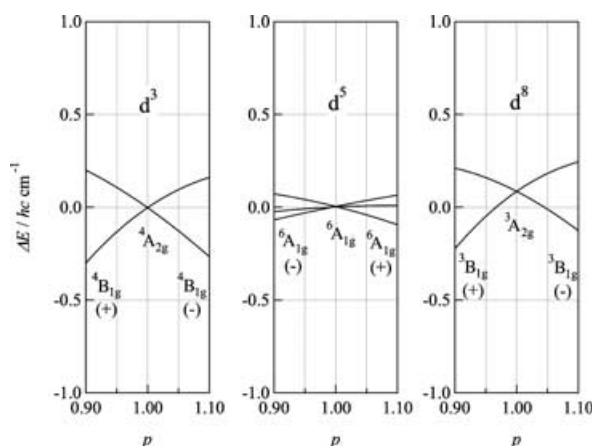


Figure 4. Energy splitting diagrams calculated for $3d^3$, $3d^5$, and $3d^8$ systems with ML_6 coordination. The parameters used in the calculations are summarized in Figure 2.

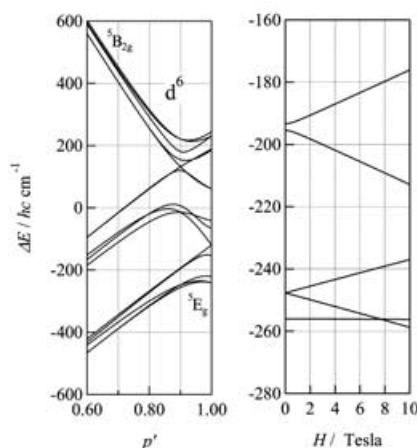
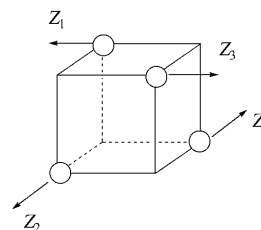


Figure 5. Left: Energy splitting diagram calculated for a six-coordinate $3d^6$ system. The axial ligand-field parameter p was fixed to 0.9 (elongated octahedron), and the variable p' changes ligand-field strength from *trans*-equatorial positions. Right: Energy splitting diagram by the applied magnetic field parallel to the equatorial axis at $p'=0.9$. The same parameters were used as in the previous calculations, except for scaled ligand-field strengths.

$x:y:z=p':1.0:p=p':1.0:0.9$. The z -elongated octahedral coordination at $p'=1.0$ becomes rhombic by lowering p' , and restores tetragonal symmetry of y -compressed octahedral coordination at $p'=0.9$. Further reduction of p' again distorts the coordination to rhombic with x -axis elongation. Zeeman splitting at $p'=0.9$ with an applied magnetic field along the y axis gave the positive D pattern with $M_s=0, \pm 1$, and ± 2 sublevels in order from the lowest energy (Figure 5, right). Further deviation to an asymmetric ligand-field strength from the equatorial ligands ($p' < 0.9$) leads to a reversal of the energy sublevels with the lowest becoming $M_s = \pm 2$ state, which corresponds to a negative D value. Care should be taken, therefore, when predicting the sign of the D value for the states that originate from ^{2S+1}E terms.

Molecules with a negative D_{mol} value: High-spin molecules composed of magnetically anisotropic metal ions can have either negative or positive D_{mol} values, and the sign of the D_{mol} value depends upon how the anisotropic metal ions are assembled in the molecule. The parameter D_{mol} is generally provided by a tensorial sum over constituent ions for a strong coupling limit,^[17] and several non-collinear molecular magnets were analyzed on this basis.^[18] More intuitive approaches useful for molecular design will be discussed here. Based on a classical vector picture, molecules with negative values of D_{mol} have two possible origins: 1) a collinear easy-axis alignment or 2) an orthogonal hard-axis alignment of a single anisotropy.^[19] We consider magnetic anisotropy of a cubane complex (so-called “metal cube”), which is a typical example of the latter case (Scheme 3). The metal cube has S_4 symmetry and four single-ion spins are ferromagnetically coupled, such that their quantization axes are mutually orthogonal.



Scheme 3. Orthogonally aligned magnetic anisotropy in a cube. Arrows represent quantization axes.

The spin Hamiltonian for this complex is given by Equation (8) in which J stands for exchange interaction between nearest neighbour spins and D is uniaxial zero-field splitting parameter for component ions. Introducing a resultant spin operator, $\hat{S} = \sum_i \hat{S}_i$, leads to Equations (9)–(11).

$$\hat{H} = -2J \sum_{i \neq j} \hat{S}_i \cdot \hat{S}_j + D(\hat{S}_{1x}^2 + \hat{S}_{2y}^2 + \hat{S}_{3x}^2 + \hat{S}_{4y}^2) \quad (8)$$

$$\hat{H} = -J(\hat{S}^2 - \sum_i \hat{S}_i^2) + \hat{H}_1 + \hat{H}_2 \quad (9)$$

$$\hat{H}_1 = \frac{D}{2} \left(\sum_i \hat{S}_i^2 - \sum_i \hat{S}_{iz}^2 \right) \quad (10)$$

$$\hat{H}_2 = \frac{D}{2} [(\hat{S}_{1x}^2 - \hat{S}_{1y}^2) - (\hat{S}_{2x}^2 - \hat{S}_{2y}^2) + (\hat{S}_{3x}^2 - \hat{S}_{3y}^2) - (\hat{S}_{4x}^2 - \hat{S}_{4y}^2)] \quad (11)$$

If only the ground-spin manifold $|S, M_s\rangle$ is considered, the first term in Equation (9) is constant, and the term \hat{H}_2 contributes only off-diagonal elements, but is not significant in the strong exchange limit ($J \gg D > 0$). Since \hat{S}_i can be substituted with $(1/4)\hat{S}$ in the large- J limit, \hat{H}_2 vanishes. Additionally, when \hat{S}_{iz} is substituted by $(1/4)\hat{S}_z$, \hat{H}_1 is then given by Equation (12) and thus, $D_{\text{mol}} = -(1/8)D$.

$$\hat{H}_1 = -(1/8)D\hat{S}_z^2 + \text{constant} \quad (12)$$

It can be expected from Equation (12) that the metal-ion assemblage with mutually orthogonal single-ion quantization axes induces a sign inversion of uniaxial magnetic anisotropy in a molecule, that is, orthogonal hard- and easy-axis alignments of the component metal ions give easy- and hard-axis anisotropy for molecules, respectively. This strategy can be extended to larger molecular systems to predict the sign of the D_{mol} values. Collinear easy-axis and orthogonal hard-axis alignments give negative D_{mol} values. Some possible spin alignments for molecules with the negative D_{mol} values are shown in Figure 6 for easy- and hard-axis components.

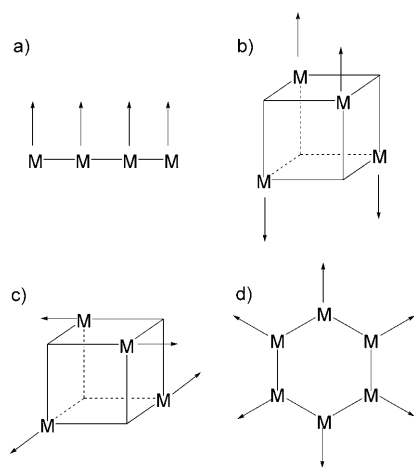


Figure 6. a,b) Collinear easy-axis ($D < 0$) and c,d) orthogonal (or radial) hard-axis ($D > 0$) alignments required for the negative D_{mol} value for molecules. Arrows in a,b) and c,d) represent easy and hard axes, respectively.

Conclusion

In the SMM $[\text{Mn}_{12}]$,^[2] each Jahn–Teller axis of the eight Mn^{III} ions is collinearly aligned in the molecule; this leads to easy-axis magnetic anisotropy for the whole molecule. In alkoxo-bridged ferrous cubes,^[3p] on the other hand, hard axis type Fe^{II} ions are assembled in the orthogonal way, and the ferrous cubes are SMMs. Although many SMMs have been prepared, they were SMMs by accident and rational synthetic strategies to control magnetic anisotropy have not yet been established. In this paper, we show how molecular anisotropy occurs when single-ion anisotropies are assembled. This work may extend choices of component metal ions beyond limited easy-axis ions and should help to design bridging ligands for assembling metal ions to be SMMs.

Acknowledgements

This work was supported by the COE and TARA projects in University of Tsukuba and by a Grant-in-Aid for Scientific Research from the Ministry of Education, Culture, Sports, Science and Technology, Japan.

- [1] a) G. Christou, D. Gatteschi, D. N. Hendrickson, R. Sessoli, *MRS Bull.* **2000**, 25, 66; b) J. R. Friedman, M. P. Sarachik, J. Tejada, R. Ziolo, *Phys. Rev. Lett.* **1996**, 76, 3830; c) L. Thomas, L. Lioni, R. Ballou, D. Gatteschi, R. Sessoli, B. Barbara, *Nature* **1996**, 383, 145; d) J. Tejada, R. F. Ziolo, X. X. Zhang, *Chem. Mater.* **1996**, 8, 1784; e) S. M. J. Aubin, N. R. Gilley, L. Pardi, J. Krzystek, M. W. Wemple, L.-C. Brunel, M. B. Maple, G. Christou, D. N. Hendrickson, *J. Am. Chem. Soc.* **1998**, 120, 4991; f) D. Ruiz, Z. Sun, B. Albela, K. Folting, G. Christou, D. N. Hendrickson, *Angew. Chem.* **1998**, 110, 315; *Angew. Chem. Int. Ed. Engl.* **1998**, 37, 300; g) H. Oshio, M. Nihei, A. Yoshida, H. Nojiri, M. Nakano, A. Yamaguchi, Y. Karaki, H. Ishimoto, *Chem. Eur. J.* **2005**, 11, 843.
- [2] a) R. Sessoli, D. Gatteschi, A. Caneschi, M. A. Novak, *Nature* **1993**, 363, 1804; b) R. Sessoli, H.-L. Tsai, A. R. Schake, S. Wang, J. B. Vincent, K. Folting, D. Gatteschi, G. Christou, D. N. Hendrickson, *J. Am. Chem. Soc.* **1993**, 115, 1804.
- [3] a) H. J. Eppley, H.-L. Tsai, N. Vries, K. Folting, G. Christou, D. N. Hendrickson, *J. Am. Chem. Soc.* **1995**, 117, 301; b) A. L. Barra, P. Debrunner, D. Gatteschi, C. E. Schulz, R. Sessoli, *Europhys. Lett.* **1996**, 35, 133; c) S. M. J. Aubin, M. W. Wemple, D. M. Adams, H.-L. Tsai, G. Christou, D. N. Hendrickson, *J. Am. Chem. Soc.* **1996**, 118, 7746; d) C. Sangregorio, T. Ohm, C. Paulsen, R. Sessoli, D. Gatteschi, *Phys. Rev. Lett.* **1997**, 78, 4645; e) Y. Pontillon, A. Caneschi, D. Gatteschi, R. Sessoli, E. Ressouche, J. Schweizer, E. Lelievre-Vera, *J. Am. Chem. Soc.* **1999**, 121, 5342; f) A. L. Barra, A. Caneschi, A. Cornia, F. Fabrizi de Biani, D. Gatteschi, C. Sangregorio, R. Sessoli, L. Sorace, *J. Am. Chem. Soc.* **1999**, 121, 5302; g) D. Gatteschi, R. Sessoli, A. Cornia, *Chem. Commun.* **2000**, 725; h) H. Andres, R. Basler, H.-U. Güdel, G. Aromi, G. Christou, H. Buttner, B. Ruffe, *J. Am. Chem. Soc.* **2000**, 122, 12469; i) A. L. Barra, D. Gatteschi, R. Sessoli, *Chem. Eur. J.* **2000**, 6, 1608; j) C. Boskovic, M. Pink, J. C. Huffman, D. N. Hendrickson, G. Christou, *J. Am. Chem. Soc.* **2001**, 123, 9914; k) A. Cornia, D. Gatteschi, R. Sessoli, *Coord. Chem. Rev.* **2001**, 219–221, 573; l) W. Wernsdorfer, N. Aliaga-Alcalde, D. N. Hendrickson, G. Christou, *Nature* **2002**, 416, 406; m) C. Boskovic, E. K. Brechin, W. E. Streib, K. Folting, J. C. Bollinger, D. N. Hendrickson, G. Christou, *J. Am. Chem. Soc.* **2002**, 124, 3725; n) J. P. Price, S. R. Batten, B. Moubarak, K. S. Murray, *Chem. Commun.* **2002**, 762; o) M. Soler, W. Wernsdorfer, K. A. Abboud, J. C. Huffman, E. R. Davidson, D. N. Hendrickson, G. Christou, *J. Am. Chem. Soc.* **2003**, 125, 3576; p) H. Oshio, N. Hoshino, T. Ito, M. Nakano, *J. Am. Chem. Soc.* **2004**, 126, 8805.
- [4] a) A. J. Tasiopoulos, A. Vinslava, W. Wernsdorfer, K. A. Abboud, G. Christou, *Angew. Chem.* **2004**, 116, 2169; *Angew. Chem. Int. Ed.* **2004**, 43, 2117; b) M. Soler, W. Wernsdorfer, K. Folting, M. Pink, G. Christou, *J. Am. Chem. Soc.* **2004**, 126, 2156; c) M. Murugesu, M. Habrych, W. Wernsdorfer, K. A. Abboud, G. Christou, *J. Am. Chem. Soc.* **2004**, 126, 4766; d) C. Cadiou, M. Murrie, C. Paulsen, V. Villar, W. Wernsdorfer, R. E. P. Winpenny, *Chem. Commun.* **2001**, 2666; e) G. L. Abbati, A. Cornia, A. C. Fabretti, A. Caneschi, D. Gatteschi, *Inorg. Chem.* **1998**, 37, 3759.
- [5] a) D. Gatteschi, A. Caneschi, L. Pardi, R. Sessoli, *Science* **1994**, 265, 1054; b) A. Müller, F. Peters, M. T. Pope, D. Gatteschi, *Chem. Rev.* **1998**, 98, 239; c) M. N. Leuenberger, D. Loss, *Nature* **2001**, 410, 789; d) S. Hill, R. S. Edward, N. Aliaga-Alcalde, G. Christou, *Science* **2003**, 302, 1015.
- [6] W. Wernsdorfer, R. Sessoli, *Science* **1999**, 284, 133.
- [7] a) M. N. Leuenberger, D. Loss, *Nature* **2001**, 410, 789; b) S. Hill, R. S. Edward, N. Aliaga-Alcalde, G. Christou, *Science* **2003**, 302, 1015.
- [8] D. Gatteschi, L. Sorace, *J. Solid State Chem.* **2001**, 159, 253.

- [9] a) P. W. Anderson, *Phys. Rev.* **1959**, *115*, 2; b) J. Kanamori, *J. Phys. Chem. Solids* **1959**, *10*, 87; c) J. B. Goodenough, *J. Phys. Chem. Solids*, **1958**, *1*, 287.
- [10] a) H. Weihe, H. U. Güdel, *Chem. Phys. Lett.* **1996**, *261*, 123; b) S. G. Brand, N. Edelstein, G. J. Hawkins, G. Shalimoff, M. R. Snow, E. R. T. Tiekink, *Inorg. Chem.* **1990**, *29*, 434; c) P. Knopp, K. Wiegardt, B. Nuber, J. Weiss, W. S. Sheldrick, *Inorg. Chem.* **1990**, *29*, 363.
- [11] a) O. Kahn, J. Galy, Y. Journaux, I. Morgenstern-Badarau, *J. Am. Chem. Soc.* **1982**, *104*, 2165; b) N. Toriha, H. Okawa, S. Kida, *Chem. Lett.* **1978**, 1269.
- [12] H. Oshio, T. Watanabe, A. Ohto, T. Ito, U. Nagashima, *Angew. Chem.* **1994**, *106*, 691; *Angew. Chem. Int. Ed. Engl.* **1994**, *33*, 670.
- [13] a) H. Oshio, N. Hoshino, T. Ito, M. Nakano, F. Renz, P. Gütllich, *Angew. Chem.* **2003**, *115*, 233; *Angew. Chem. Int. Ed.* **2003**, *42*, 223; b) H. Oshio, Y. Saito, T. Ito, *Angew. Chem.* **1997**, *109*, 2789; *Angew. Chem. Int. Ed. Engl.* **1997**, *36*, 2673; c) H. Oshio, N. Hoshino, T. Ito, *J. Am. Chem. Soc.* **2000**, *122*, 12602.
- [14] A. Abragam, B. Bleaney, *Electron Paramagnetic Resonance of Transition Ions*, Oxford University Press, Oxford, **1970**, Section 19.2.
- [15] a) B. N. Figgis, M. A. Hitchman, *Ligand Field Theory and Its Applications*, Wiley-VCH, Weinheim, **2000**, Chapter 3; b) T. Schönher, *Top. Curr. Chem.* **1997**, *191*, 88; c) P. E. Hoggard, *Coord. Chem. Rev.* **1986**, *70*, 85; d) A. B. P. Lever, *Inorganic Electronic Spectroscopy*, 2nd ed., Elsevier, Tokyo, **1984**; e) E. Larsen, G. N. La Mar, *J. Chem. Educ.* **1974**, *51*, 633; f) J. K. Burdett, *Molecular Shapes*, Wiley, New York, **1980**.
- [16] a) E. I. Solomon, A. B. P. Lever, *Inorganic Electronic Structure and Spectroscopy, Vol. 1*, Wiley, New York, **1999**; b) A. Bencini, I. Ciof-
ni, and M. G. Uytterhoeven, *Inorg. Chim. Acta* **1998**, *274*, 90; c) H. Schilder, H. Lueken, *J. Magn. Magn. Mater.* **2004**, *281*, 17; d) R. Boca, *Coord. Chem. Rev.* **2004**, *248*, 757.
- [17] a) A. Bencini, D. Gatteschi, *Electron Paramagnetic Resonance of Exchange Coupled Systems*, Springer, Berlin, Tokyo, **1990**, Sections 3.2 and 4.3; b) A. Abragam, B. Bleaney, *Electron Paramagnetic Resonance of Transition Ions*, Oxford University Press, Oxford, **1970**, Section 19.2. c) C. J. Ballhausen, *Introduction to Ligand Field Theory*, MacGraw-Hill, New York, **1962**, Section 6g.
- [18] a) A. Cornia, M. Affronte, A. G. M. Jansen, G. L. Abbati, D. Gatteschi, *Angew. Chem.* **1999**, *111*, 2409; *Angew. Chem. Int. Ed.* **1999**, *38*, 2264; b) O. Waldmann, J. Schüle, R. Koch, P. Müller, I. Bernt, R. W. Saalfrank, H. P. Andres, H. U. Güdel, and P. Allenspach, *Inorg. Chem.* **1999**, *38*, 5879; c) O. Waldmann, R. Koch, S. Schromm, J. Schüle, P. Müller, I. Bernt, R. W. Saalfrank, F. Hampel, and E. Balthes, *Inorg. Chem.* **2001**, *40*, 2986; d) G. L. Abbati, L.-C. Brunel, H. Casalta, A. Cornia, A. C. Fabretti, D. Gatteschi, A. K. Hassan, A. G. M. Jansen, A. L. Maniero, L. Pardi, C. Paulsen, U. Segre, *Chem. Eur. J.* **2001**, *7*, 1796; e) D. Collison, V. S. Oganessian, S. Piligkos, A. J. Thomson, R. E. P. Winpenny, E. J. L. McInnes, *J. Am. Chem. Soc.* **2003**, *125*, 1168.
- [19] a) M. Nakano, G. Matsubayashi, T. Muramatsu, T. C. Kobayashi, K. Amaya, J. Yoo, G. Christou, D. N. Hendrickson, *Mol. Cryst. Liq. Cryst.* **2002**, *376*, 405; b) E.-C. Yang, D. N. Hendrickson, W. Wernsdorfer, M. Nakano, L. N. Zakharov, R. D. Sommer, A. L. Rheingold, M. Ledeza-Gairaud, and G. Christou, *J. Appl. Phys.* **2002**, *91*, 7382.

Published online: June 20, 2005